A STUDY OF THE EFFECT OF INITIAL MICROSTRUCTURE ON SUBSTRUCTURE STRENGTHENING CHARACTERISTICS IN AN ALUMINUM CONDUCTOR ALLOY

A THESIS

Presented to

The Faculty of the Division of Graduate Studies

By

David Michael Bowden

In Partial Fulfillment

of the Requirements for the Degree

Master of Science in Metallurgy

Georgia Institute of Technology

June, 1978

A STUDY OF THE EFFECT OF INITIAL MICROSTRUCTURE ON SUBSTRUCTURE STRENGTHENING CHARACTERISTICS IN AN ALUMINUM CONDUCTOR ALLOY

Approved:

Bruce G. LeFevre, Chairman

Edgar A. Starke, Jr.

Pieter Muijderman

Date Approved by Chairman 5/30/78

ACKNOWLEDGMENTS

The author wishes to express his sincerest appreciation to his advisor, Dr. Bruce G. LeFevre, the most patient man in the world, for his many contributions to the work performed for this thesis. Also, the helpful comments of the reading committee members, Dr. Edgar A. Starke, Jr., and Dr. Pieter Muije, are greatly appreciated.

I am greatful to the Southwire Company, of Carrolton, Georgia, for providing the material used in this study, and for their help in material processing.

I am also greatful to the Georgia Institute of Technology for providing financial support during the course of this study.

I would also like to thank my fellow graduate students, and my parents, Mr. and Mrs. Herbert M. Bowden, Jr., for their help and encouragment during the course of this work.

TABLE OF CONTENTS

LIST OF TABLES

LIST OF ILLUSTRATIONS

Figure Page

Figure Page

SUMMARY

The effect of initial microstructure on substructure strengthening characteristics in an Al-0.6Fe-0.2Cu (wt. %) conductor alloy subjected to room temperature wire drawing to large strains was studied. The dilute alloy was compared to 99.99% pure aluminum. Two initial microstructures were used; an "F" temper, representing the structure of the as-cast and hot rolled rod, and an "O" temper, produced by annealing the "F" temper rod at 800°F for 3 hours. Stress strain curves were obtained at various intervals of wire drawing, and structures were characterized by optical metallography and transmission electron microscopy (TEM).

The Al-Fe-Cu alloy and 99.99% aluminum develop well-defined substructures during wire drawing. Initial microstructure has little effect on substructure development and the subsequent strengthening effect of the substructure in pure aluminum. However, the strengthening effect of subgrains in the Al-Fe-Cu alloy is affected by the initial rod microstructure. Prior tempering affects the formation of subgrain boundaries, and thus the nature of these boundaries. The modified Hall-Petch relation for substructure strengthening varies with prior tempering. The "F" temper alloy is found to strain harden more rapidly than either the "O" temper alloy or the pure aluminum in either temper. The Hall-Petch line for the "F" temper alloy has a steeper slope, indicating the greater strengthening effect of the cell boundaries.

CHAPTER I

INTRODUCTION

The economic advantages of using aluminum to transmit electrical power are significant. However, electrical conductor grade (EC) aluminum has inadequate mechanical properties to meet requirements imposed by service conditions in electrical applications. Consequently, considerable effort has been devoted to the development of higher strength aluminum conductor alloys.

For aluminum conductor alloys, it is necessary to satisfy the requirements for conductivity, strength, ductility, and thermal stability (creep resistance). The conventional methods of strengthening aluminum, such as work hardening, solid solution strengthening, and precipitation hardening, are unacceptable for electrical applications since they result in materials that are either thermally unstable, or have poor conductivity[1]. However, metals of high stacking fault energy such as aluminum develop well-defined substructures during deformation, and substructure strengthening may be used as the mechanism to obtain the necessary properties of strength and conductivity in these alloys.

Recent studies have centered on correlating the degree of substructure development, i.e. cell or subgrain size, with mechanical properties. Very little has been done to determine the effect of

initial rod microstructure on substructure development during wire drawing, and subsequent strain hardening characteristics. The purpose of this investigation is to provide a better understanding of how initial rod microstructure affects work hardening behavior during heavy cold drawing. Specifically, the effects of microstructure are examined in terms of:

a. The effect of initial microstructure on substructure development during wire drawing.

b. The effect of initial microstructure on strain hardening characteristics during wire drawing.

These effects are examined for both high purity aluminum and an Al-0.6Fe-0.2Cu conductor alloy. The effects of alloying will be examined in terms of:

a. The effect of precipitates on substructure development and subsequent strengthening.

b. The effect of alloying on differences in substructure strengthening behavior due to differences in initial rod microstructure.

Differences in substructure strengthening characteristics are examined by establishing strain hardening curves and Hall-Petch type relationships for each material.

CHAPTER II

LITERATURE REVIEW

Substructure Development

A dislocation substructure is formed in alloys as a result of recovery. The basic mechanisms of recovery in metals involve the movement of dislocations created during plastic deformation into cell or subgrain boundaries. If this process occurs during deformation, it is called dynamic recovery. The tendency for dislocations to form a cell structure is quite strong in many metals and exists over a wide temperature range.

The role of dynamic recovery is not the same in all metals. It occurs most readily in metals of high stacking fault energy. This fact indicates that the primary mechanism involved in dynamic recovery is thermally activated cross slip[(2)].

Various models have been proposed relating dynamic recovery to the formation of cell structures. With increasing strain dislocations multiply and form tangles, with the result that a cellular substructure gradually develops which saturates with respect to dimensions. The detailed dislocation arrangements which make up cell walls are quite complex, but certain features are evident. Most important is that cell walls are typically low-angle boundaries, characterized by relatively high boundary dislocation densities. A second feature of importance is that long range stresses appear to be low in both cell and subgrain

structures. Several investigators, most notably Holt[3] and Kuhlmann-Wilsdorf[4-8] have used mathematical models to describe the behavior of dislocation arrays in the development of cells.

When deformation is continued to large enough strains or at high enough temperatures that significant dynamic recovery can occur, marked increases in boundary perfection are observed. The boundary perfection gives subgrains much of the character of high angle grains, although the misorientations are less than those of grains.

The distinction made between dislocation cells and subgrains lies in the extent to which the substructure is developed. If the processing conditions are such that cross slip and dislocation climb may occur more readily, a more sharply defined subgrain structure will result.

It is important to realize in any discussion of substructure development that there are qualitative differences between the substructural units formed in creep, in hot working at high strain rates, or at low temperatures in cold working. Generally, the largest subgrains develop in creep, at low strain rates, and have sharp refined walls of substantial misorientation, while smaller size cells develop at low temperatures. These cells, like the fine units produced by rapid hot working, tend to contain wider boundaries with appreciable dislocation densities and smaller misorientations[9].

Thus, strain rate is important (creep vs. hot-work) as well as deformation temperature. The total strain is important at low temperatures, since misorientation increases with strain[10,11],

especially when cross slip is easy.

In the next section, the characteristics of substructures will be considered in terms of their strengthening behavior.

Substructure Strengthening Behavior

The effect of grain boundaries on the yield strength of metals can be described by the Hall-Petch relationship[12-14]:

$$\sigma = \sigma_0 + k_1(d)^{-1/2} \tag{1}$$

where σ is the yield strength, σ_0 is the friction stress that opposes the motion of mobile dislocations in the matrix, d is the grain size, and k_1 is a constant that is related to the strength of the grain boundaries.

This expression has been extended to materials with substructures. Thompson, Baskes and Flanagan[15] relate flow stress to the dislocation density ρ, as follows:

$$\sigma = \sigma_0 + \alpha G b \rho^{1/2} \tag{2}$$

where G is the shear modulus, b the Burgers vector, and α is a constant referred to as the dislocation strengthening efficiency[16]. Models have been developed which relate average cell size to dislocation density, as in the following equation:

$$d = k_2/\rho^{1/2} \tag{3}$$

Substitution of (3) into (2) gives a relationship between flow stress and average cell size:

$$\sigma = \sigma_0 + k_3 d^{-1} \tag{4}$$

A more generalized expression may be written as:

$$\sigma = \sigma_0 + k_4 d^{-m} \tag{5}$$

A range of m values has been reported for various alloys, depending on the type of deformation and the deformation temperature. Data for substructures produced at relatively low temperatures tends to correlate well with equation (5), with a value of -1 for m. Langford and Cohen[10], Rack and Cohen[17], and Young and Sherby[18], all studying iron and iron based alloys, show a linear correlation of σ with $(d)^{-1}$. Staker and Holt[19] found the same correlation with copper, as have Fujita and Tabata[20] with high purity aluminum.

The strengthening behavior of high temperature subgrains may be described by the Hall-Petch relation of equation (1). Rack and Cohen[21] have shown this to be the case for heavily deformed iron alloys. Data from the review paper of McElroy and Szkopiak[16] on aluminum, iron, and iron based alloys also correlate well with $(d)^{-1/2}$.

The nature of the substructure, and thus the yield strength,

depends on such variables as deformation temperature and strain rate. Rack and Cohen[21] have shown, for example, that in the case of heavily deformed iron wire, m of equation (5) varies from 1 to 1/2 as the recovery temperature is increased. Dislocation cells and subgrains simply represent the extremes of the types of substructure, and thus the strengthening effect, that can be produced.

Effect of Alloying on Substructure Development

There are two ways in which alloy additions may aid in the development and stabilization of a fine substructure. Solid solution additions can help by their effect on the stacking fault energy and the ability to tie up defects, thus hindering dislocation motion and dynamic recovery. The second method involves the formation of fine precipitates to control subgrain size.

Solid solution additions can aid in stabilizing substructures. One effect of solute atoms is their tendency to inhibit the growth of dislocation networks by the mechanism of solute drag[16]. In materials of medium stacking fault energy, segregation of solute atoms to dislocations and other defects such as vacancies takes place, effectively lowering the stacking fault energy. Solid solution additions also aid in the generation of dislocations, leading to a higher dislocation density for a given amount of deformation. Cell formation may be accelerated, thus producing a finer substructure[22].

In the development of suitable conductor alloys, conductivity is the primary criterion to be considered. Solid solution additions may

significantly increase the resistivity of the material. Figure 1 shows that solid solution additions over one weight percent will significantly increase the resistivity of EC grade aluminum. For conductor alloys, the formation of fine precipitates is used to aid the development and stabilization of a fine substructure. The primary requirement of the precipitate particles is that they are thermodynamically stable and will not dissolve or coarsen during subsequent processing. In these materials, the subgrain size is a function of the particle spacing[24-26]. The particles aid in the generation of dislocations, and the pinning effect of the particles aids in stabilizing the substructure, and in making it finer.

Effect of Processing on Substructure Development

For alloy systems in which a dispersion of fine precipitates is used to obtain a fine substructure, control of the casting operation is important. In the casting operation the precipitates form between dendrites upon solidification. It is difficult to obtain an even particle dispersion if the cooling rate is slow and the dendrites are coarse. However, rapid solidification of the casting will produce finer dendrites, and thus give a smaller particle spacing. The finer the initial particle dispersion, the finer and more homogeneous the substructure that can be produced with further processing. Thus rapid solidification of the casting will produce a particle dispersion more effective in producing a fine substructure. Further deformation, such as rolling the cast ingot into rod and drawing the rod into wire,

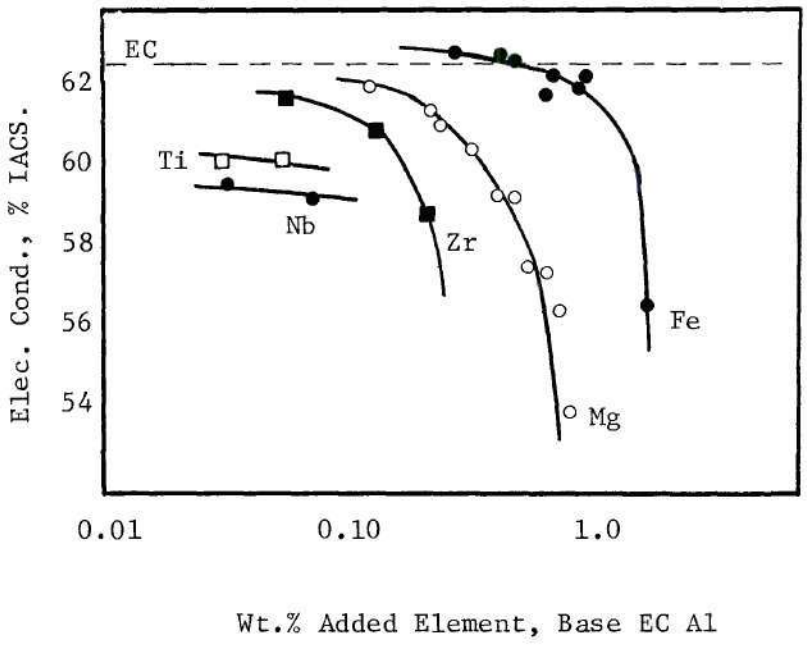

Figure 1. Effect of Alloy Additions on the Electrical Conductivity of EC Grade Aluminum.[19]

will break up and string out the particles, producing a more uniform structure. The rate of deformation becomes important in that the more deformation that is achieved per pass, the more uniform that deformation will be in terms of its effect on the substructure. The deformation temperature is important for its effect on strengthening behavior as discussed in the previous section. At extremely high temperatures, the possibility of recrystallization exists. It has been shown for aluminum, however, that extensive dynamic recovery during hot working prevents recrystallization. Post deformation annealing can, of course, induce static recrystallization, depending on the annealing time and temperature. In this case, recrystallization begins by subgrain boundary coalescence, producing large subgrains of high misorientation. Recrystallization proceeds when these high angle boundaries begin to migrate.

During the wire drawing operation, a great deal of heat is generated due to friction between the die and workpiece. A cooling fluid, usually an oil of some type, is used to disipate the heat. Care should be taken to insure proper use of the cooling fluid to prevent any static recrystallization from occuring between wire drawing stages.

In summary, to obtain the maximum strengthening effect, a fine, homogeneous substructure must be produced. The ability to achieve this depends on the quality of the structure resulting from previous processing steps. Just as the rod substructure depends on the cast structure of the ingot, the substructure of the final wire product depends on the quality of the rod substructure. At each step in the

process, the object is to produce as fine and homogeneous a structure as possible.

The Al-Fe-Cu System

Figure 2[27] shows the aluminum corner of the Al-Fe-Cu ternary phase diagram. For alloys containing less than one percent copper and iron, the material consists of $FeAl_3$ precipitates in a matrix of aluminum. The copper is predominantly in solid solution with the aluminum. However, $FeAl_3$ can dissolve limited amounts of copper, producing $(FeCu)Al_6$. An extensive range for $FeAl_3$ shown in the phase diagram probably includes some $(FeCu)Al_6$. The solubility of neither iron or copper in aluminum is reduced in the ternary alloy, but since copper lowers the eutectic point, the maximum amount of iron soluble in aluminum decreases.

Iron additions to aluminum increase the strength up to about one percent iron. Above one percent, forgeability and rollability are reduced. Iron increases the resistivity of aluminum 2.56 micro-ohm-cm/% iron when in solution, but only 0.058 micro-ohm-cm/wt.% iron when in the form of a precipitate phase.

Copper is added also to improve strength. However, the electrical resistivity increases almost proportionally to the quantity of dissolved copper to a value of 4.5×10^{-8} ohm-cm. at the solubility limit of 5.7% copper. As the copper content is increased, there is a continuous increase in the hardness, but strength and especially ductility depend on whether the copper is in solid solution or exists in the form of

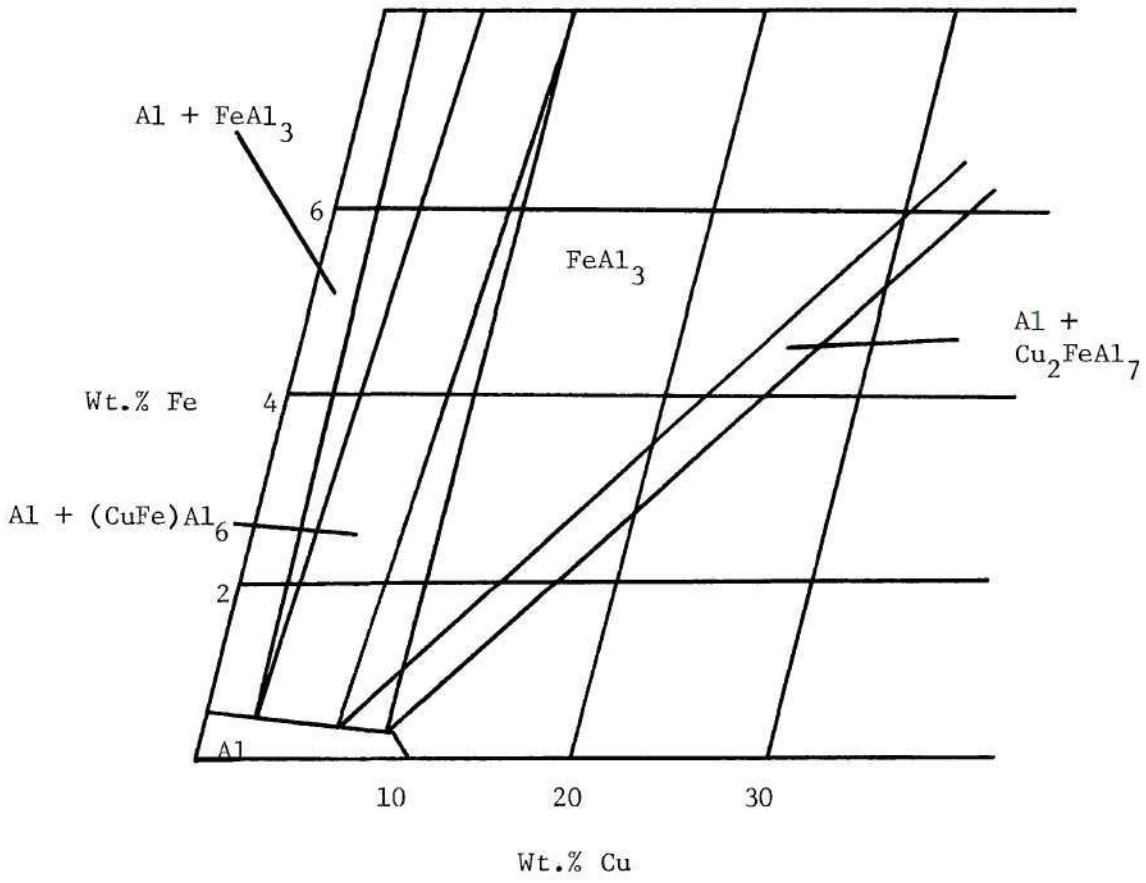

Figure 2. Aluminum Corner of the Al-Fe-Cu Phase Diagram.[2]

precipitates. Dissolved copper produces the highest increase in strength while retaining substantial ductility. Copper also improves the creep resistance of aluminum, but there is no general agreement on whether copper is more effective in this when in solid solution or in the precipitate phase.

In summary, the ternary alloy that best satisfies the requirements of a conductor alloy would be one that contains small (less than one weight percent) additions of iron and copper. Iron additions will form the stable $FeAl_3$ precipitates, although some $(CuFe)Al_6$ may exist. These particles will be useful in producing and stabilizing a fine substructure necessary for strengthening the wire product.

CHAPTER III

EXPERIMENTAL PROCEDURES

Material for this study was provided by the Southwire Company of Carrolton, Georgia. Both 99.99% pure aluminum and Al-0.6Fe-0.2Cu alloy, were provided in the form of continuously cast and hot rolled 3/8 inch diameter rod, produced by the Southwire Company's SCR Mill continuous rod system.

Two initial rod microstructures were used, one using the as-cast and hot rolled rod as recieved, and the second an equiaxed grain structure produced by fully annealing the as recieved rod for three hours at 800°F, and air cooling. Standard Aluminum Association designations for these two conditions, which will be used here, are "F" temper for the as fabricated (continuously cast and hot rolled) condition, and "O" temper for the annealed condition. From these two rod conditions, wires of various reductions were produced for both pure aluminum and the ternary alloy using a bench scale wire drawing machine, with a die string-up as shown in Table 1. Wires were drawn at a rate of 42 feet per minute. Heating of the wires during drawing was minimized by the continuous flow of lubricant oil at the inlet tip of the die.

Optical Metallography

After each reduction in the drawing process, a sample was

Table 1. Wire Drawing Parameters

Drawing Reduction No.	Die Diameter (in.)	Cross Sectional Area(sq.in.)	Percent Reduction in Area	True Strain
1	0.380	0.1134	0	0
2	0.325	0.083	26.0	0.313
3	0.288	0.065	42.0	0.554
4	0.258	0.052	53.0	0.775
5	0.230	0.042	63.0	1.004
6	0.203	0.032	71.0	1.254
7	0.182	0.026	77.0	1.472
8	0.162	0.021	81.0	1.705
9	0.144	0.016	86.0	1.941
10	0.114	0.010	92.0	2.410
11	0.102	0.0082	93.0	2.630

obtained for metallographic observation. Transverse and longitudinal sections were observed to determine the effects of wire drawing on the grain structure. Samples were mounted in quick mount in order to minimize the heating involved in the conventional bakelite mounting. Samples were ground through 600 grit silicon carbide paper, and polished through 1.0 and 0.3 micron alumina. The final polish was performed on a vibramet using 0.05 micron magnesium oxide.

A light, 30 second etch, consisting of 0.5% hydrofluoric acid in water, was used to reveal the precipitates.

Grain structure was revealed by anodizing. A lead cathode was used in a solution of 4.5 ml. fluoboric acid in 95.5 ml. water, with a potential of 20 volts for a period of 90 seconds. To obtain the best results, the solution should be stirred continuously. Good results were indicated by a pink color on the metal surface. The grain structure was revealed when the sample was viewed under polarized light.

Transmission Electron Microscopy

Transmission electron microscopy (TEM) was used to record the dislocation substructure on specimens prepared after each reduction in the wire drawing process. Thin transverse sections were cut from each reduction. These thin sections were mounted on an aluminum block using two-sided tape, to provide a way to hold them, and to insure that they were ground flat. It was necessary to grind evenly on both sides to obtain the best results. Specimens were ground through 600 grit

silicon carbide paper to a thickness of 0.01 inches. From this thin wafer, specimens 2.3 mm. in diameter were punched out using a special tool. These samples were further thinned using a jet polishing apparatus. A solution of 75% methanol and 25% nitric acid was used with a potential of 300 volts. Samples were thinned equally from both sides. The appropriate polishing time was determined by polishing completely through one sample and determining the rate of material removal from the original sample thickness and time of polishing. The final preparation was an electropolish using the same methanol-nitric acid solution, cooled to -20°C with a bath of methanol and dry ice. A stainless steel cathode was used at a potential of 14 volts. A light was placed directly behind the sample, and the sample was polished until a hole appeared, as evidenced by the light visible through the sample.

Thin foils were observed in a Siemens Elmiskop 1A electron microscope operated at 100 kV.

Average subgrain size was measured by use of the linear intercept method on TEM photomicrographs. At least 300 cells were counted for each reduction, and at least two samples of each reduction were examined.

Tensile Testing

Tensile tests were conducted on an Instron machine (model FDLM), operated at a crosshead speed of 2 mm/min. A strain gage extensometer with a two inch gage length was used for the determination of stress-strain curves. A minumum of three curves with failure inside the gage length were obtained for each reduction in wire drawing.

CHAPTER IV

RESULTS AND DISCUSSION

The strain hardening and substructural changes during wire drawing of high purity aluminum and Al-0.6Fe-0.2Cu alloy are discussed in this section. Differences in the behavior of pure aluminum and the ternary alloy are related to the effects of alloying. The effects of rod microstructure are examined by comparing the "F" and "O" tempers of each material.

Optical Metallography

The first objective of the optical metallography was to observe any differences in precipitate distribution in wires produced from the two alloy rod conditions. Photomicrographs showing the precipitate distributions in wires produced from the "F" temper condition are shown in Figures 3 and 4, and for wires produced from the "O" temper alloy rod in Figures 5 and 6. There are no obvious differences between wires produced from these two conditions, either in the number of particles or in particle size. The distributions appear to be even throughout the wires, with no variations from edge to center. This is as would be expected, since the primary requirement of the precipitate phase is that it be thermally stable.

Grain structure variations with increasing strain are shown for wires produced from the F-temper alloy rod in Figures 7-14, and for

the "O" temper alloy wires in Figures 15-22. For the "F" temper condition, the structure is dendritic, as shown by both transverse and longitudinal sections. The dendrites form first at the surface of the casting, where solidification begins, and grow inward to the center. Although wire drawing breaks up this initial structure, the dendritic characteristics are still evident in the final wire product.

The series of photomicrographs of the "O" temper wires shows the effects of non-uniform deformation. Grains near the surface undergo more deformation than those near the center of the wire. Consequently, those near the surface are broken up more, resulting in a finer grain structure near the surface in the wires. However, with increasing strain, this effect becomes less and less, and the microstructure of the final wire product is fairly uniform. As in the "F" temper condition, wire drawing to large strains breaks up the rod structure. Grains become elongated in the wire drawing direction, with smaller transverse cross sectional areas.

Transmission Electron Microscopy

The substructure of the two rod conditions and wires produced from them for both pure aluminum and the ternary alloy were studied by transmission electron microscopy (TEM) of thin foils taken transverse to the wire axis.

TEM photomicrographs of the initial rod conditions for the alloy are shown in Figures 23 and 24. The "F" temper alloy rod shows a well defined substructure, produced during the hot rolling stage.

This substructure is characterized by distinct subgrain boundaries. Annealing this structure to produce the "O" temper rod gives the structure shown in Figure 24. The "O" temper rod has a large, fairly subgrain-free recrystallized structure. Precipitates are also visible in this structure. As mentioned in Chapter II, the precipitates form interdendritically upon solidification of the casting. The particles form in groups, or colonies. A typical precipitate colony is shown in Figure 25. Photomicrographs of substructures for several reductions from the rod are shown in Figures 26-28 for the "F" temper alloy, and in Figures 29-31 for the "O" temper alloy. In both cases, wire drawing produces a finer substructure with increasing strain.

Figure 32 shows plots of average linear intercept length as a function of strain for both pure aluminum and the Al-Fe-Cu alloy. A comparison of the alloy with pure aluminum shows the effect of the precipitates in producing and stabilizing a fine substructure. In both "F" and "O" tempers, the alloy has a finer substructure than the pure aluminum drawn to the same total strain. This holds for both tempers, as would be expected due to the stability of the precipitate phase.

In the case of pure aluminum, it appears that initial rod microstructure has little effect on either the rate of substructure development or on cell size attainable by wire drawing. Curves for both "F" and "O" tempers tend to fall within the same range. However, this is not the case for the alloy. There is a large initial difference in the rate of substructure refinement. Although there is a large initial difference in the substructures of the two rod conditions,

it appears that the ultimate cell size attainable by wire drawing to large strains is roughly the same for both tempers. The difference in rate of cell refinement compensates for the large initial differences in the rod. This behavior, which is different than that found in the pure aluminum, can only be attributed to the effect of alloying, since the processing conditions were identical for both pure aluminum and the alloy. This difference between pure aluminum and the alloy can be explained in terms of the rod substructure developed during hot rolling. In the case of the alloy, a fairly well developed substructure is found in the hot rolled rod, due to the ability of the precipitates to aid in the generation of dislocations to form subgrains. Annealing fails to eliminate these effects, and thus produces the differences found between the "O" temper pure aluminum and the "O" temper alloy.

Strengthening Behavior

Strain hardening curves for both pure aluminum and the ternary alloy in both "F" and "O" tempers are shown in Figure 33. Pure aluminum has lower strength in both tempers, and strain hardens at roughly the same rate in both conditions. Annealing shifts the curve downward slightly from the "F" temper curve, without changing the strain hardening characteristics.

For the alloy, the two conditions show significantly different strain hardening characteristics, with the F temper condition hardening at a much higher rate. The maximum yield stress attainable in the "F" temper alloy is higher than the "F" temper pure aluminum

by roughly one hundred percent. The strain hardening rate of the "F" temper alloy is also greater than that of the "F" temper pure aluminum, as shown by the steeper slope of the strain hardening curve. This is explainable in terms of the degree of substructure refinement in the alloy rod, as compared to that of the pure aluminum rod. Since the "F" temper alloy rod has a well developed substructure as a result of rolling, the strengthening effect of the cells is felt immediately upon further working (drawing). The pure "F" temper rod requires further deformation by drawing to develop an equivalent substructure, and thus its strength level falls below that of the "F" temper alloy. Annealing the "F" temper alloy rod to produce the "O" temper condition significantly lowers the yield stress, although the "O" temper alloy is stronger than the pure aluminum in either condition. It appears that annealing washes out much of the difference in strain hardening rate between the alloy and pure aluminum, as the curve for the "O" temper alloy has the same general curvature as that for pure aluminum. The "F" temper alloy rod has a fairly well developed subgrain structure, and the strengthening effect of the cells is felt immediately with further working. Annealing to produce the "O" temper eliminates this substructure, and thus a certain amount of deformation is required to again develop a substructure before its strengthening effect becomes apparent. For this reason, the slope of the initial portion of the curve is less for the "O" temper alloy than that of the "F" temper condition.

The one remaining question to be answered is whether the

strengthening effect of the substructure is independent of temper. If the strength of the metal is the same for a given subgrain size regardless of temper, then it may be said that temper has no effect on the ability of subgrains to strengthen the metal. Figure 34 shows the effect of subgrain size on the yield strength. The relative strengthening effects of alloying and substructure formation can be interpreted from this diagram. Values of σ_0 and k from these lines are shown in Table 2, and compared to those values for several other aluminum alloys. The strengthening due to alloying alone can be determined by upward shifts in the lines, with no change in slope. The slope of the line can be interpreted as a measure of the relative effect of substructure on strengthening. If two lines are parallel, it may be said that they exhibit the same substructure strengthening characteristics. Any differences in strength level would be due to alloying. For example, the lines representing "O" temper pure Al and "O" temper alloy are roughly parallel. Thus, subgrains have the same strengthening effect in both materials, and the difference in strength may be attributed to the alloy additions. The "F" temper alloy has a much steeper slope than the "O" temper alloy. In this case, subgrains have a greater contribution to strength in the "F" temper condition. This is due to the fact that the substructure of the "F" temper rod is much more developed than that of the "O" temper rod, and thus substructure effects are more immediately felt in the strengthening behavior. Annealing the "F" temper alloy washes out the substructure effect, and thus the line representing the "O" temper alloy is roughly

parallel to that of pure aluminum. This was shown previously in the strain hardening curves of Figure 32, where the "O" temper alloy was shown to strain harden at the same rate as the pure aluminum.

The specific nature of the cell boundary strengthening may be considered in terms of the particles providing a network of pinning sites for dislocations, in which case the observed k value would include not only the normal strength of a subgrain boundary in pure aluminum, but the effect of a dispersed particle network as well. This would account for the higher k value for the "F" temper alloy. Annealing to produce the "O" temper alloy lowers the observed value of k to that of pure aluminum. Since annealing has no effect on the stable precipitate phase, the lower k value must be attributed to a change in the nature of the subgrain boundaries themselves. The interaction of a dispersed insoluble second phase and an initial fine substructure results in a higher work hardening rate and more effective cell boundary strengthening even though the rate of cell refinement with strain is less. A complete understanding of the nature of the boundaries requires a more detailed knowledge of the deformation mechanisms involved in their formation.

(a)

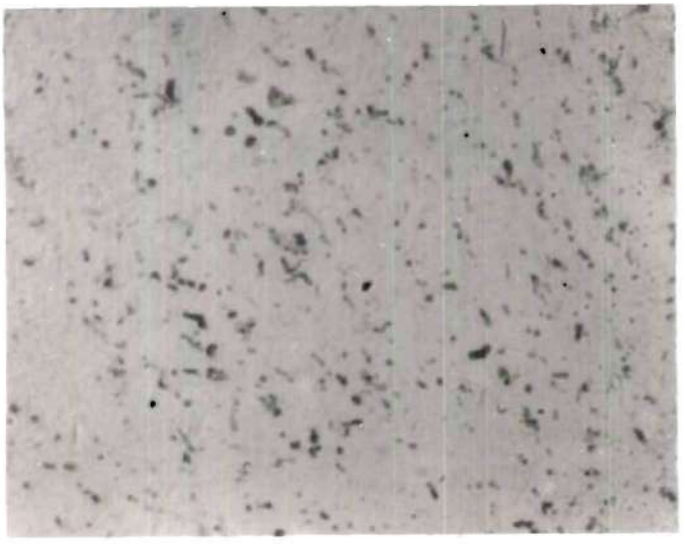

(b)

Figure 3. Effect of Drawing on Precipitate Distribution in "F" Temper Alloy: (a) 0.380 in. dia. rod; (b) 0.288 in. dia. Wire; 1000X.

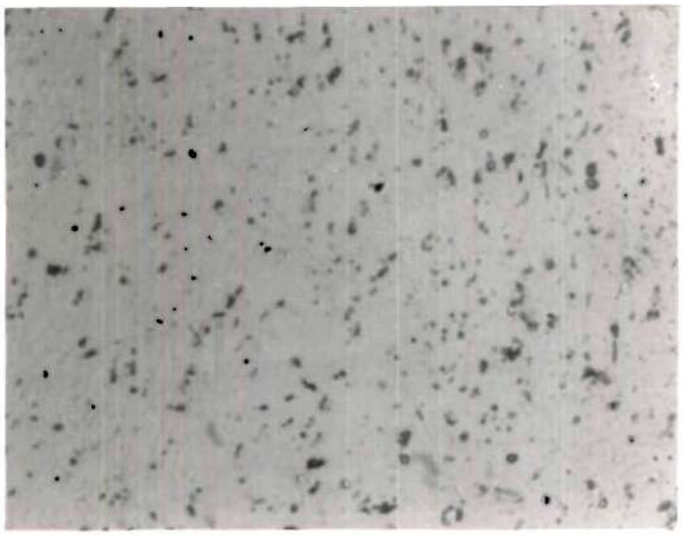

(a)

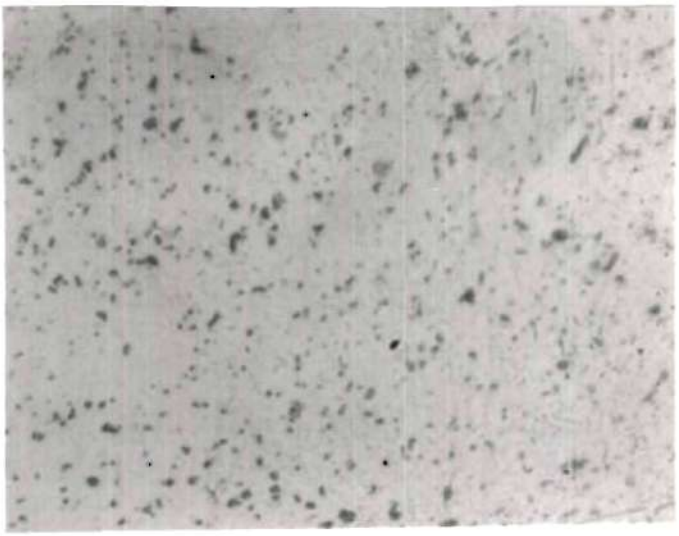

(b)

Figure 4. Effect of Drawing on Precipitate Distribution in "F" Temper Alloy: (a) 0.182 in. dia; (b) 0.102 in. dia. Wire; 1000X.

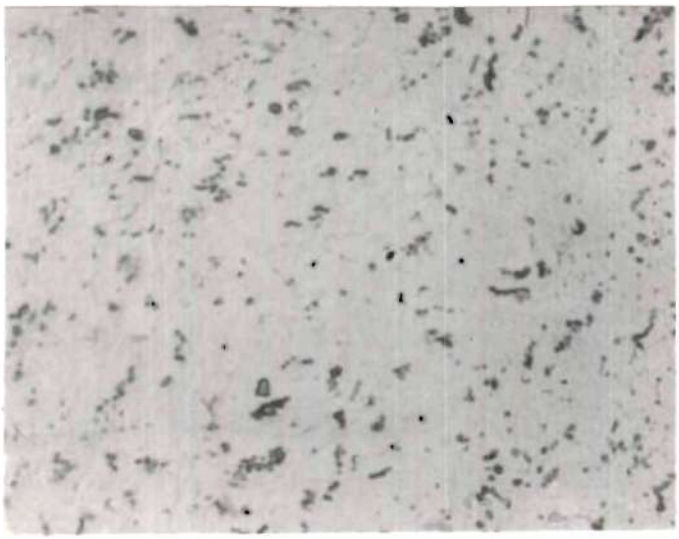

(a)

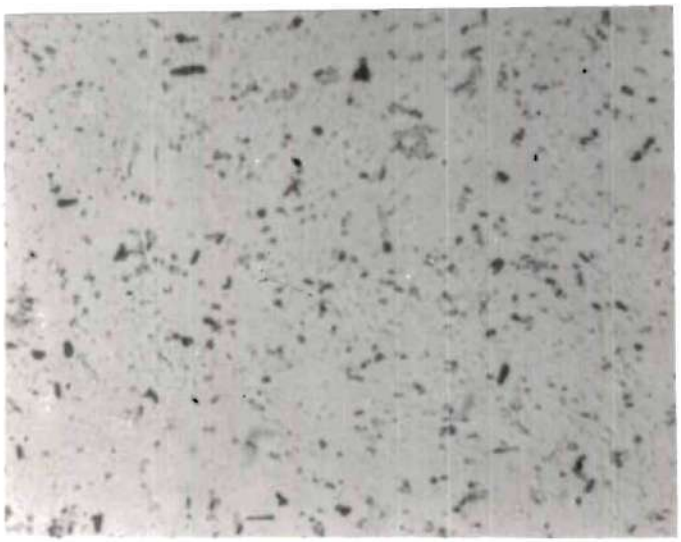

(b)

Figure 5. Effect of Drawing on Precipitate Distribution in "O" Temper Alloy: (a) 0.380 in. dia. Rod; (b) 0.288 in. dia. Wire; 1000X.

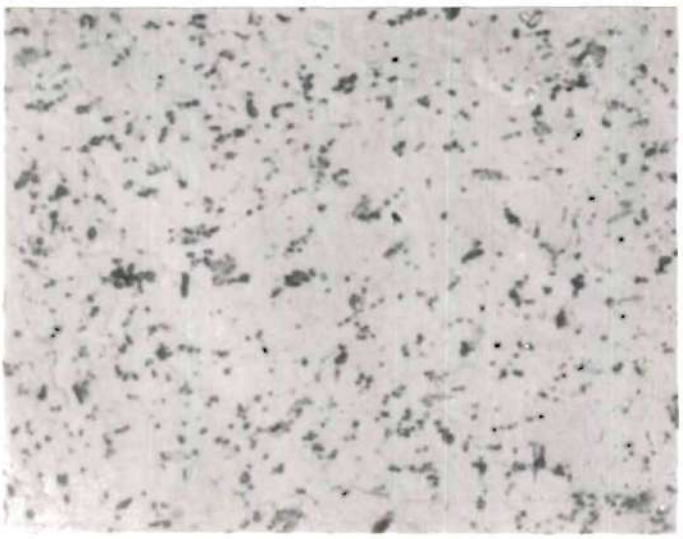

(a)

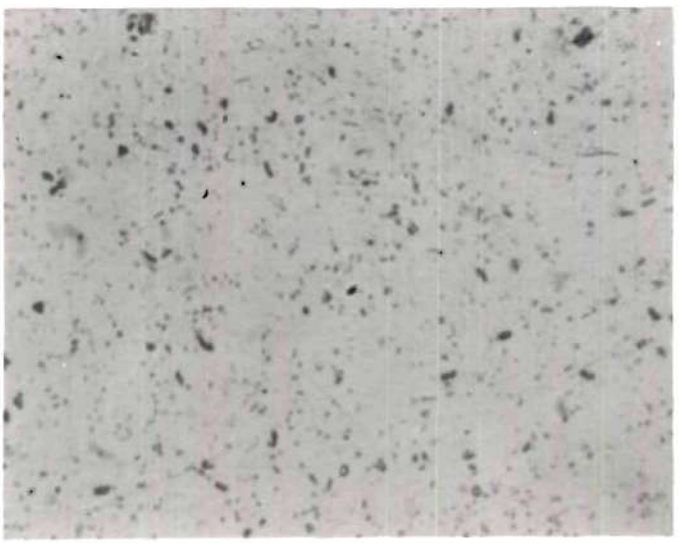

(b)

Figure 6. Effect of Drawing on Precipitate Distribution in "O" Temper Alloy: (a) 0.182 in. dia.; (b) 0.102 in. dia. Wire; 1000X.

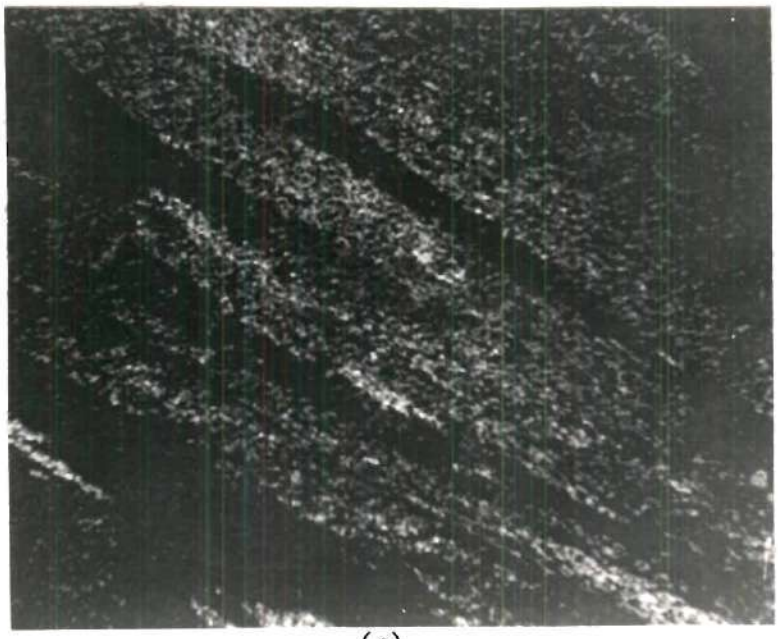

(a)

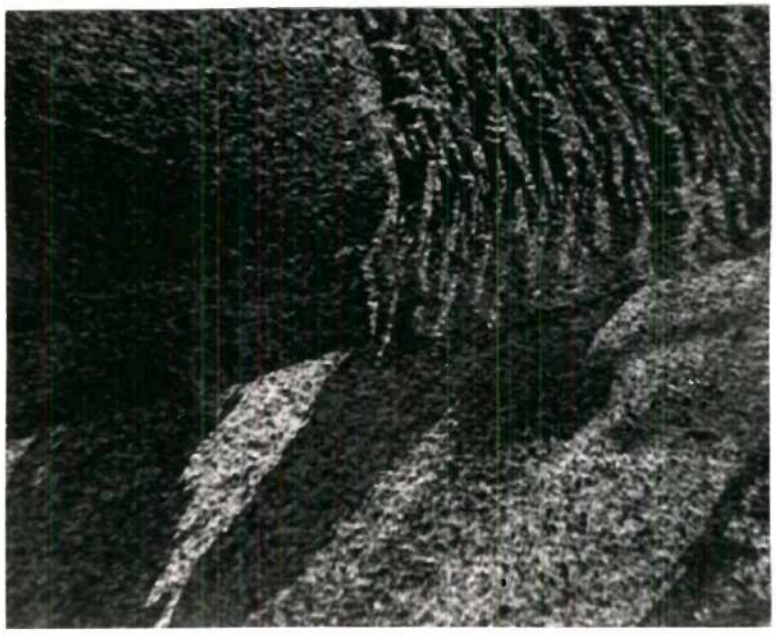

(b)

Figure 7. Transverse Grain Structure, "F" Temper Alloy Rod: (a) Edge; (b) Center; 60X.

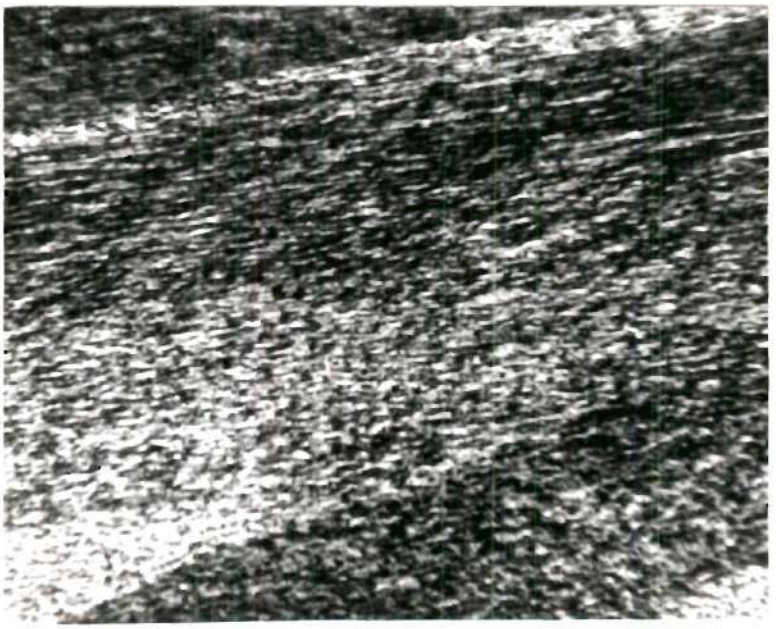

(a)

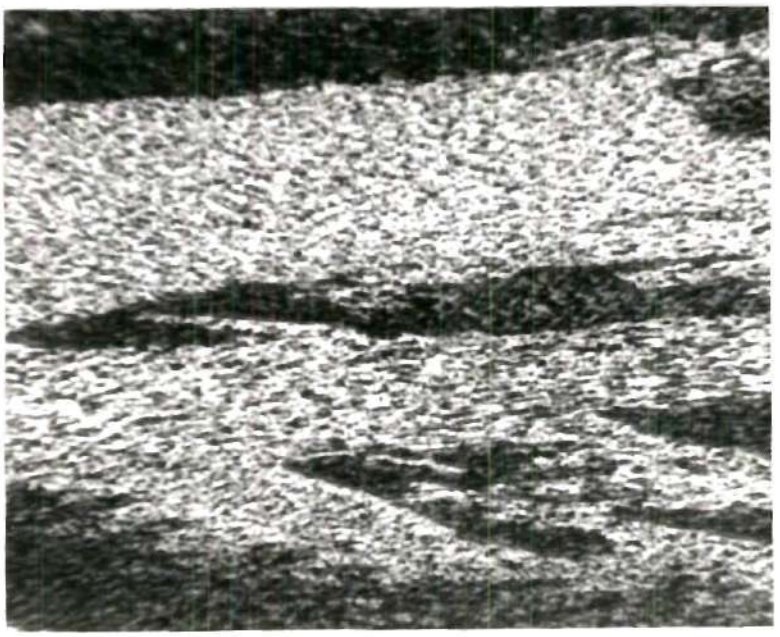

(b)

Figure 8. Longitudinal Grain Structure, "F" Temper Alloy Rod: (a) Edge; (b) Center; 60X.

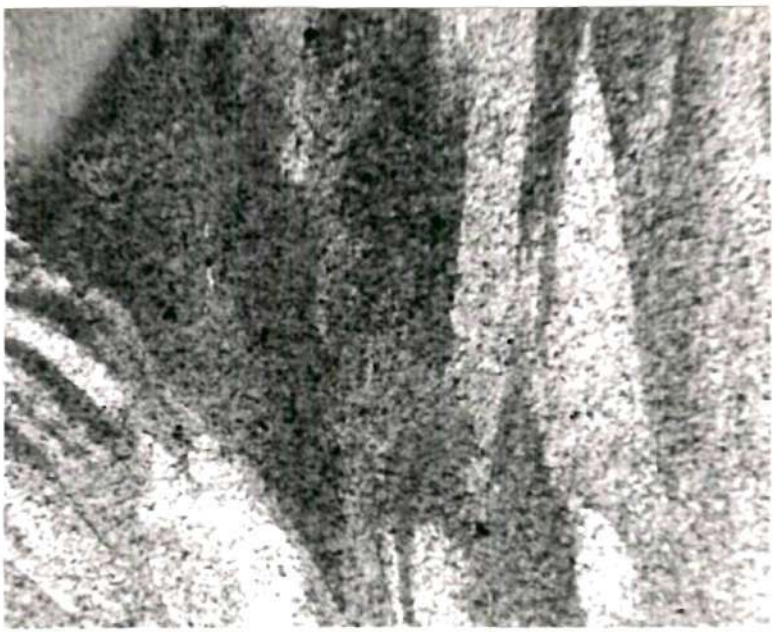

(a)

(b)

Figure 9. Transverse Grain Structure, "F" Temper 0.288 in. dia. Alloy Wire: (a) Edge; (b) Center; 60X.

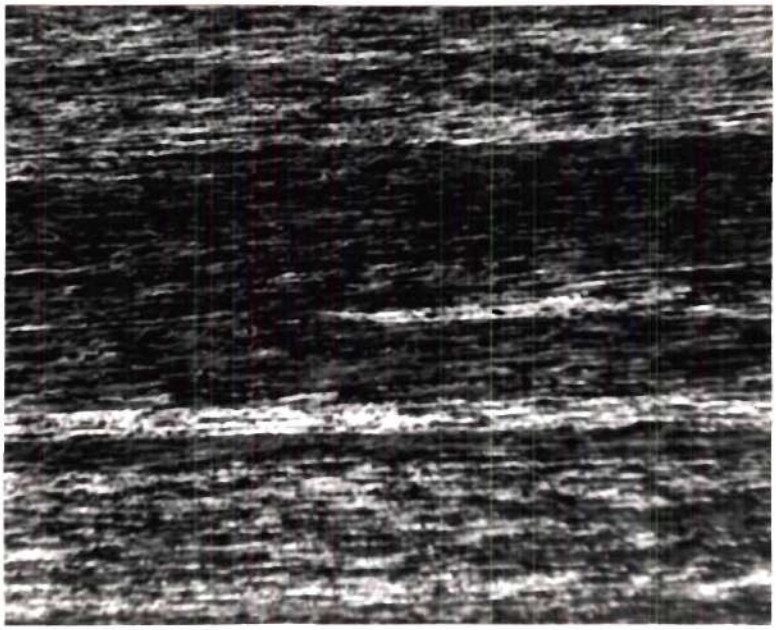

(a)

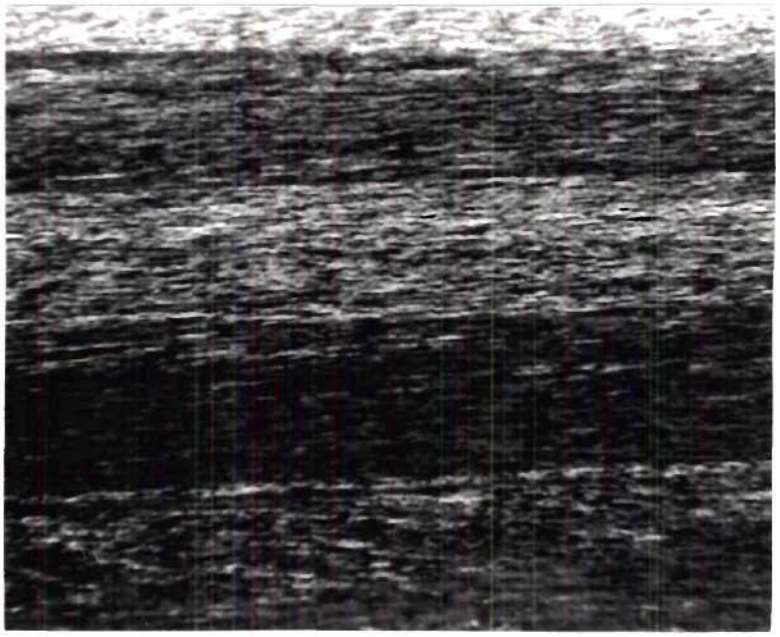

(b)

Figure 10. Longitudinal Grain Structure, "F" Temper 0.288 in. dia. Alloy Wire: (a) Edge; (b) Center; 60X.

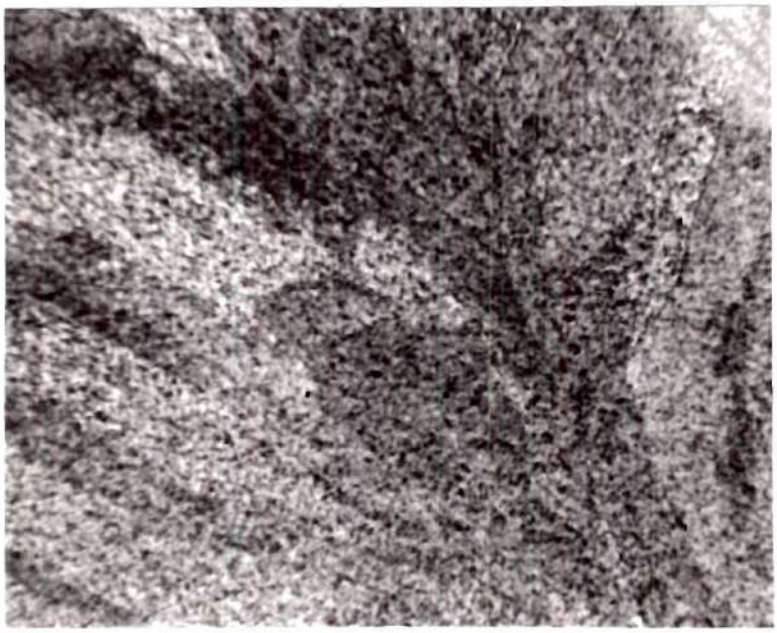

Figure 11. Transverse Grain Structure, "F" Temper 0.182 in. dia. Alloy Wire, Edge to Center; 60X.

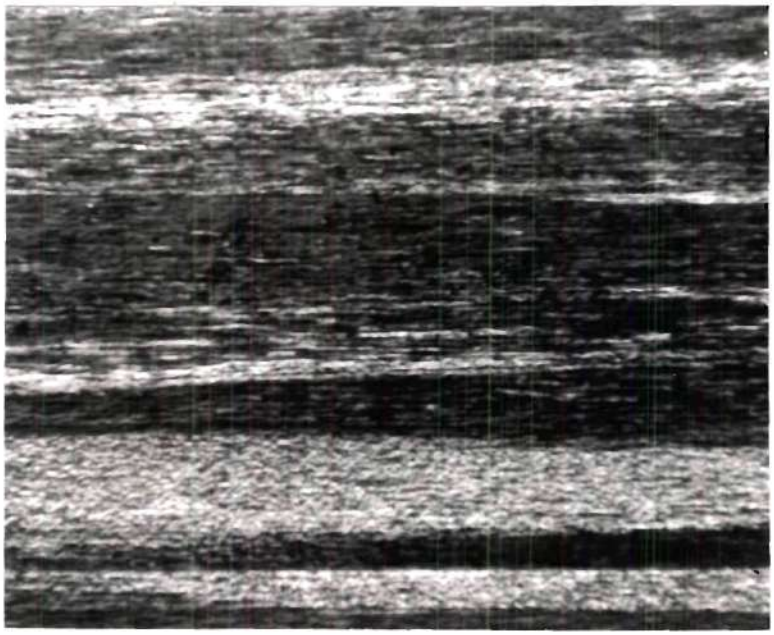

Figure 12. Longitudinal Grain Structure, "F" Temper 0.182 in. dia. Alloy Wire, Edge to Center; 60X.

Figure 13. Transverse Grain Structure, "F" Temper 0.102 in. dia. Alloy Wire, Edge to Edge; 60X.

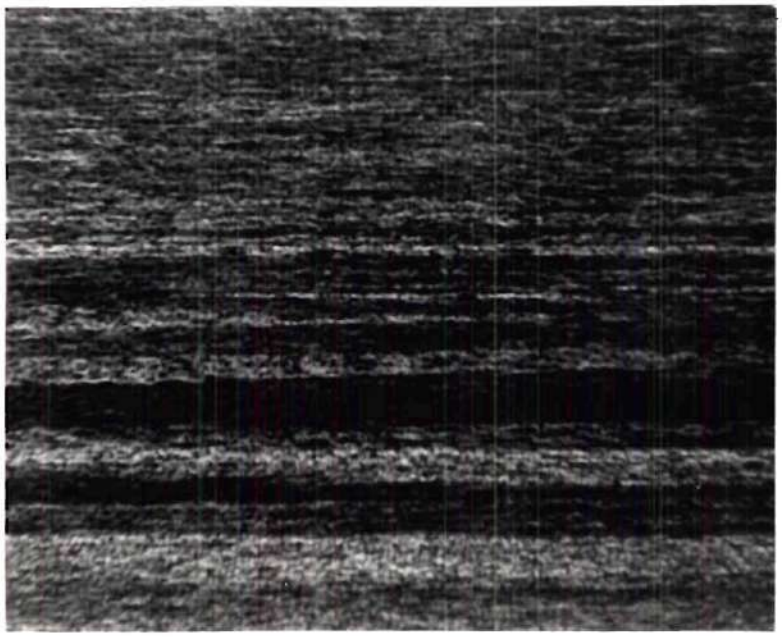

Figure 14. Longitudinal Grain Structure, "F" Temper 0.102 in. dia. Alloy Wire, Edge to Edge; 60X.

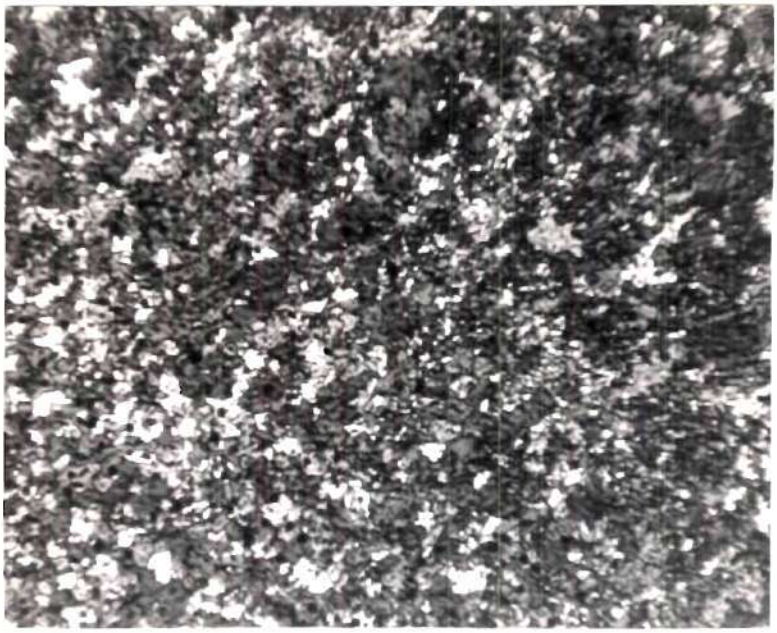

(a)

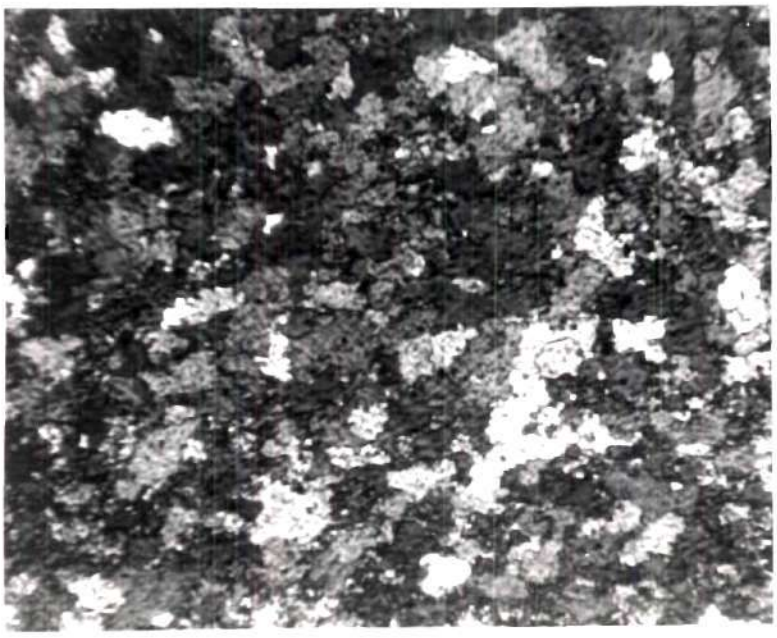

(b)

Figure 15. Transverse Grain Structure, "O" Temper Alloy Rod: (a) Edge; (b) Center; 60X.

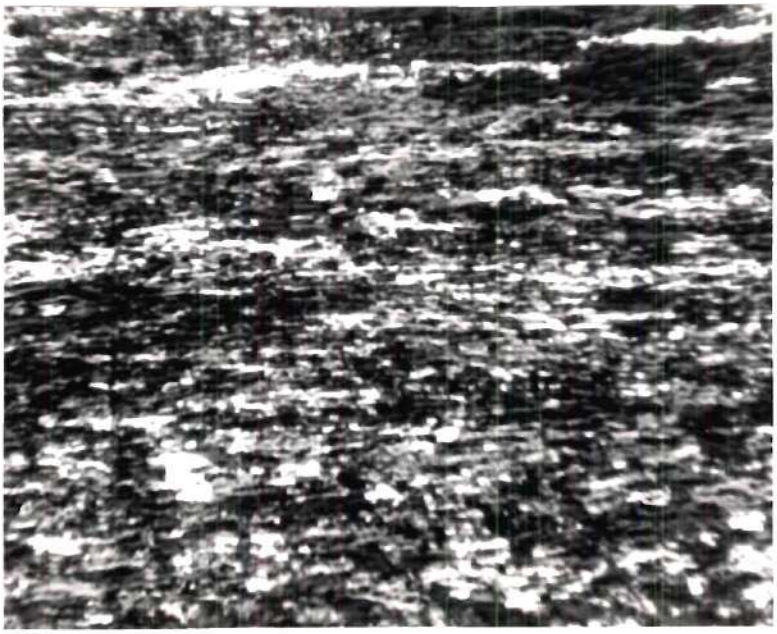

(a)

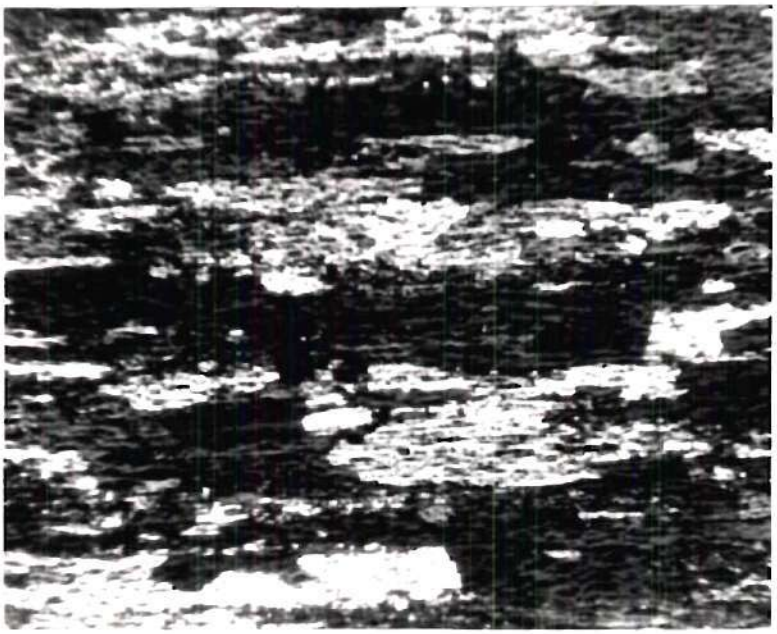

(b)

Figure 16. Longitudinal Grain Structure, "O" Temper Alloy Rod: (a) Edge; (b) Center; 60X.

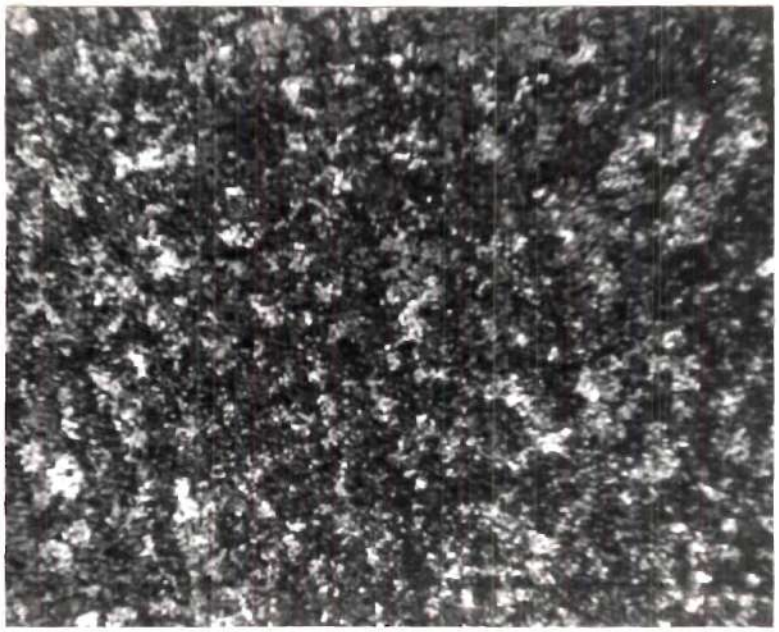

(a)

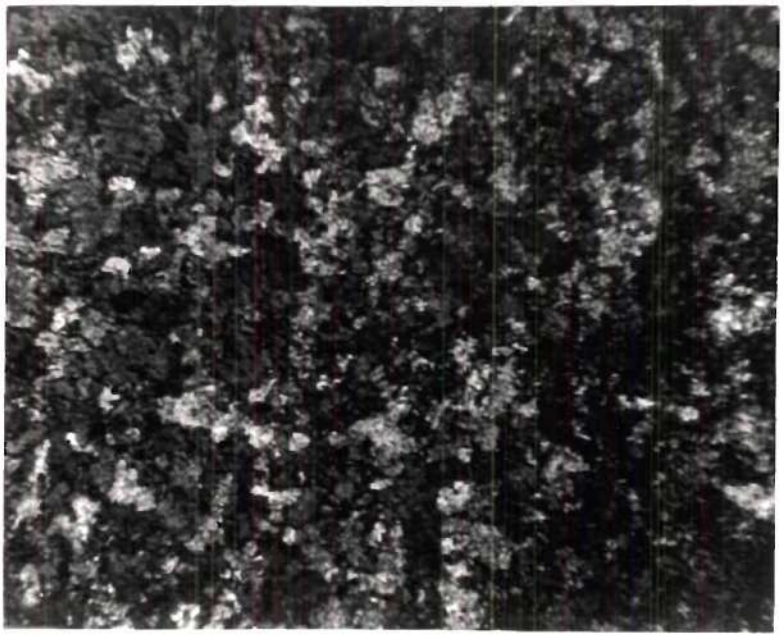

(b)

Figure 17. Transverse Grain Structure, "O" Temper 0.288 in. dia. Alloy Wire: (a) Edge; (b) Center; 60X.

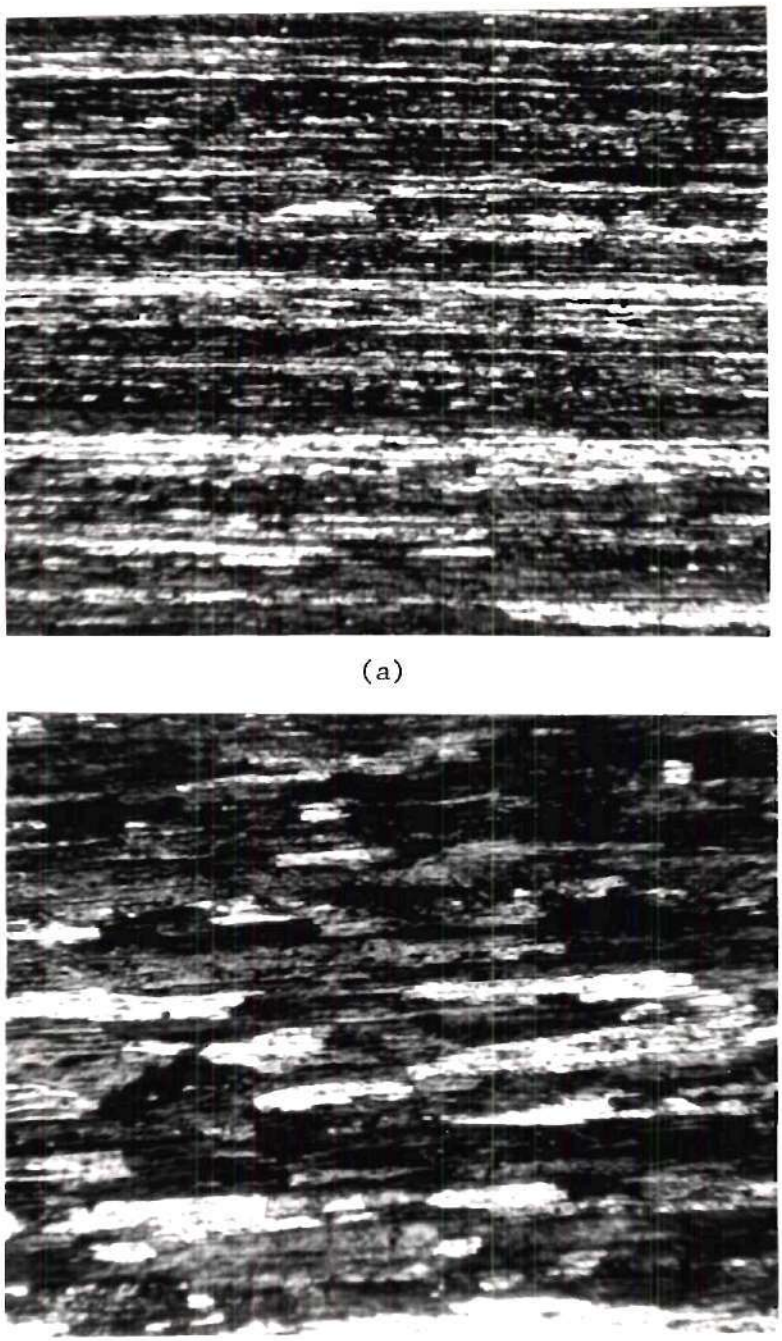

(a)

(b)

Figure 18. Longitudinal Grain Structure, "O" Temper 0.288 in. dia. Alloy Wire: (a) Edge; (b) Center; 60X.

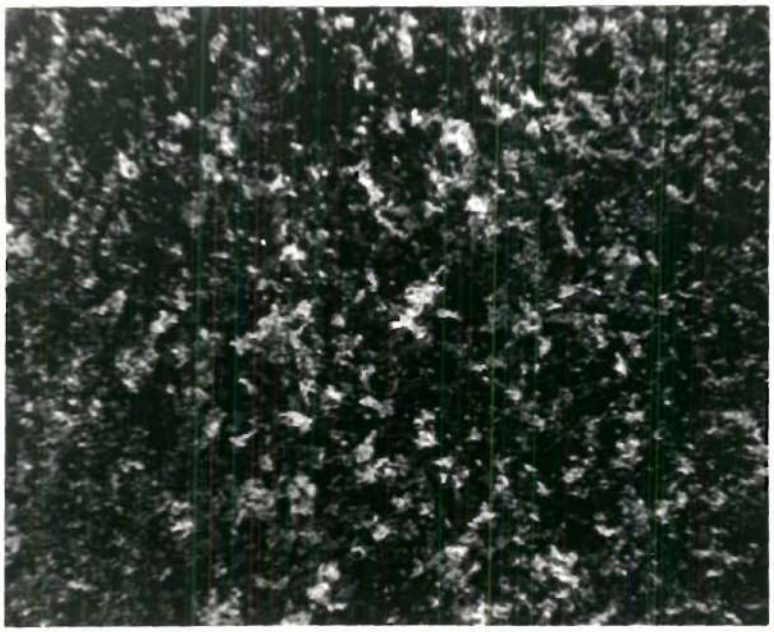

Figure 19. Transverse Grain Structure, "O" Temper 0.182 in. dia. Alloy Wire, Edge to Center; 60X.

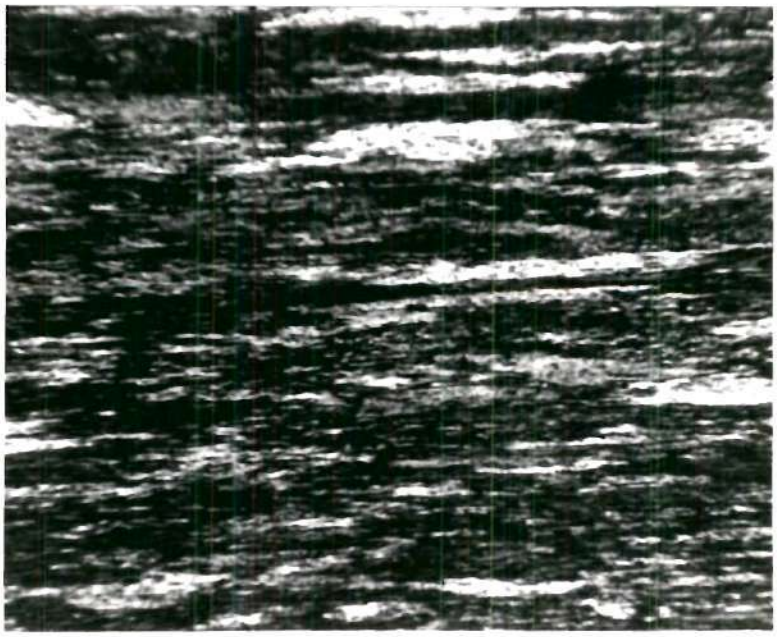

Figure 20. Longitudinal Grain Structure, "O" Temper 0.182 in. dia. Alloy Wire, Edge to Center; 60X.

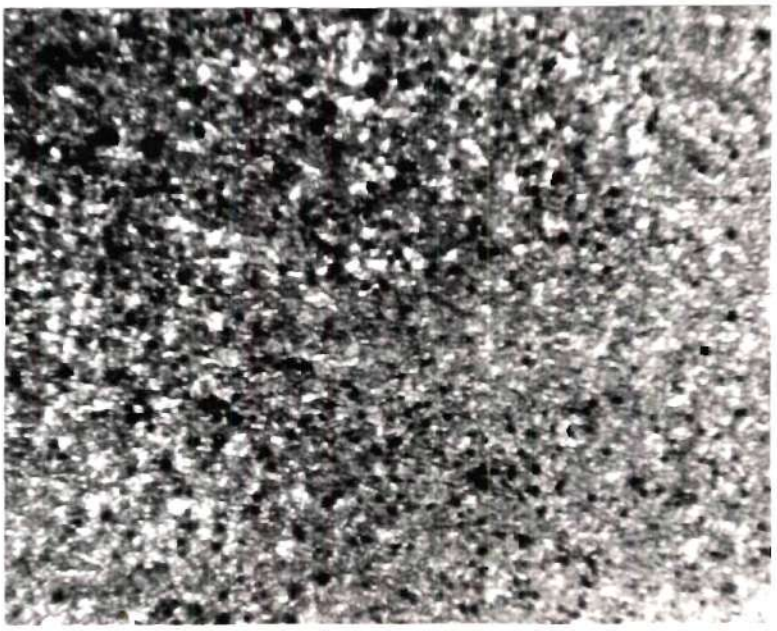

Figure 21. Transverse Grain Structure, "O" Temper 0.102 in. dia. Alloy Wire, Edge to Edge; 60X.

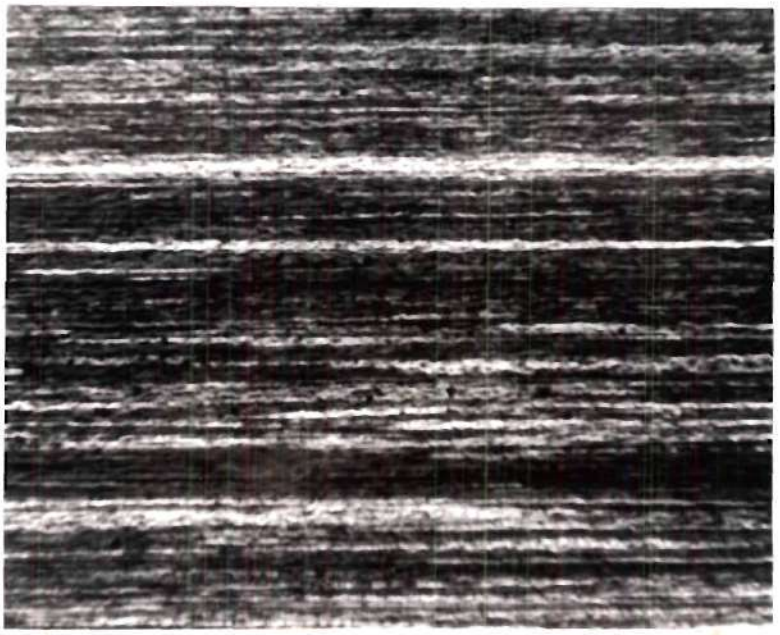

Figure 22. Longitudinal Grain Structure, "O" Temper 0.102 in. dia. Alloy Wire, Edge to Edge; 60X.

Figure 23. Transmission Electron Micrograph of "F" Temper 0.380 in. dia. Rod; 16,000X.

Figure 24. Transmission Electron Micrograph of "O" Temper 0.380 in. dia. Alloy Rod; 16,000X.

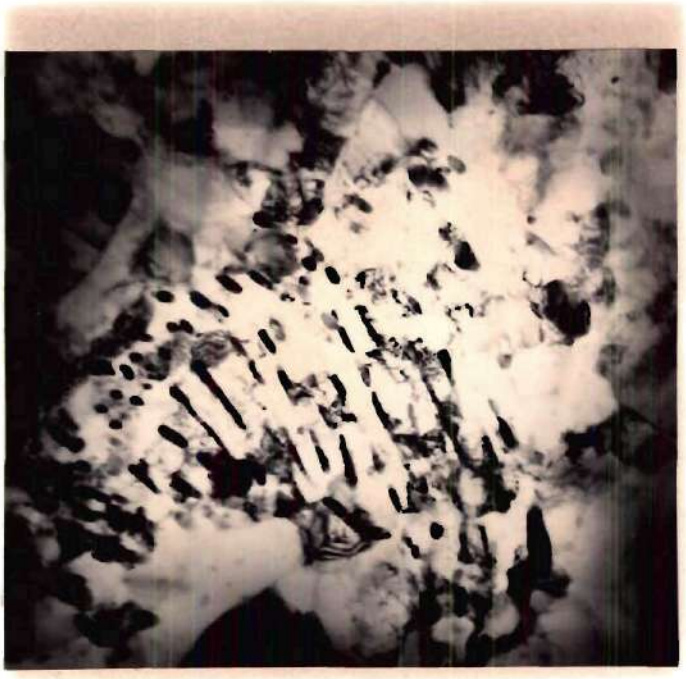

Figure 25. Transmission Electron Micrograph of "F" Temper Alloy Rod, Showing a Typical Precipitate Colony; 16,000X.

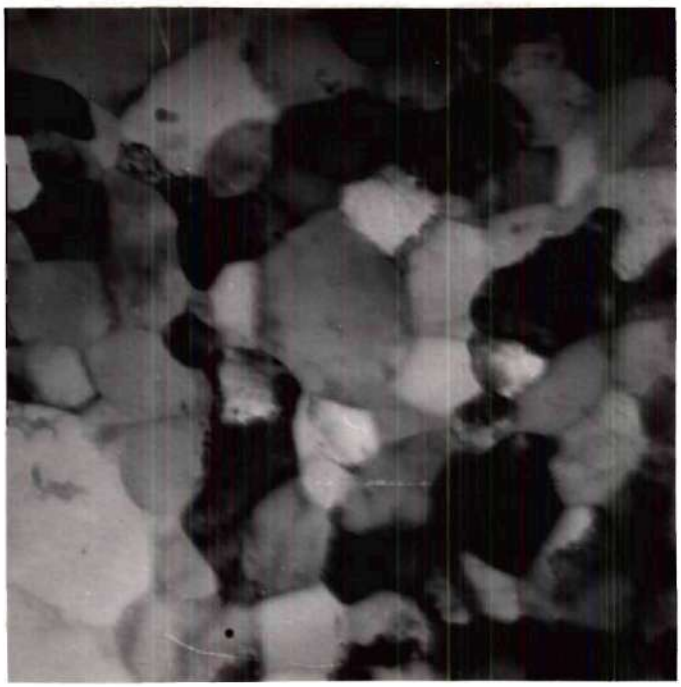

Figure 26. Transmission Electron Micrograph of "F" Temper 0.288 in. dia. Alloy Wire; 20,000X.

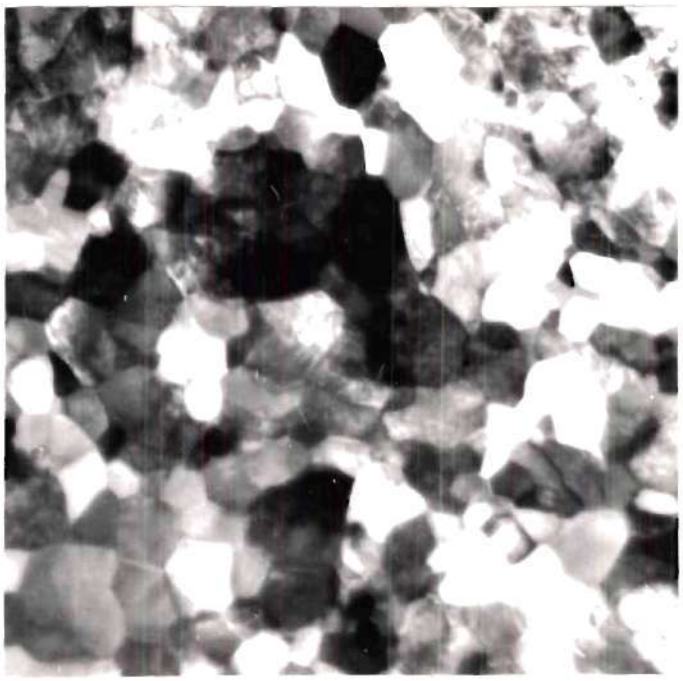

Figure 27. Transmission Electron Micrograph of "F" Temper 0.182 in. dia. Alloy Wire; 20,000X.

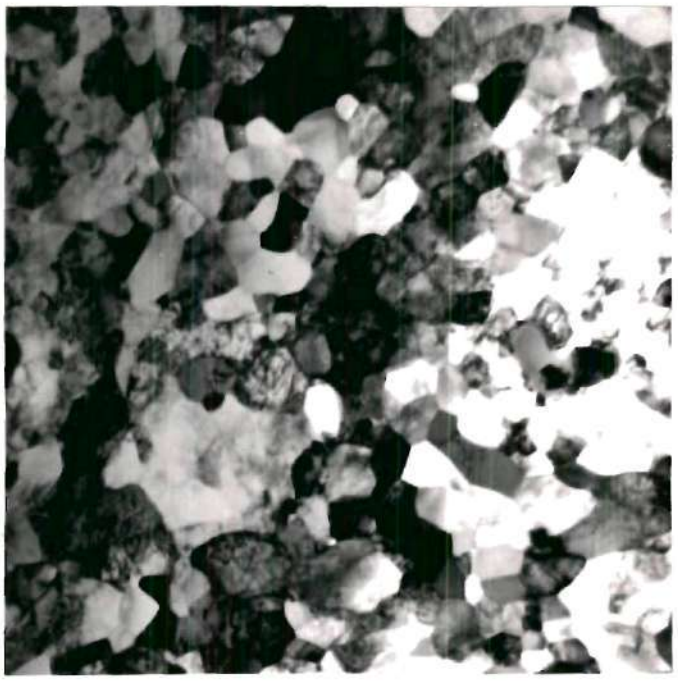

Figure 28. Transmission Electron Micrograph of "F" Temper 0.102 in. dia. Alloy Wire; 20,000X.

Figure 29. Transmission Electron Micrograph of "O" Temper 0.288 in. dia. Alloy Wire; 20,000X.

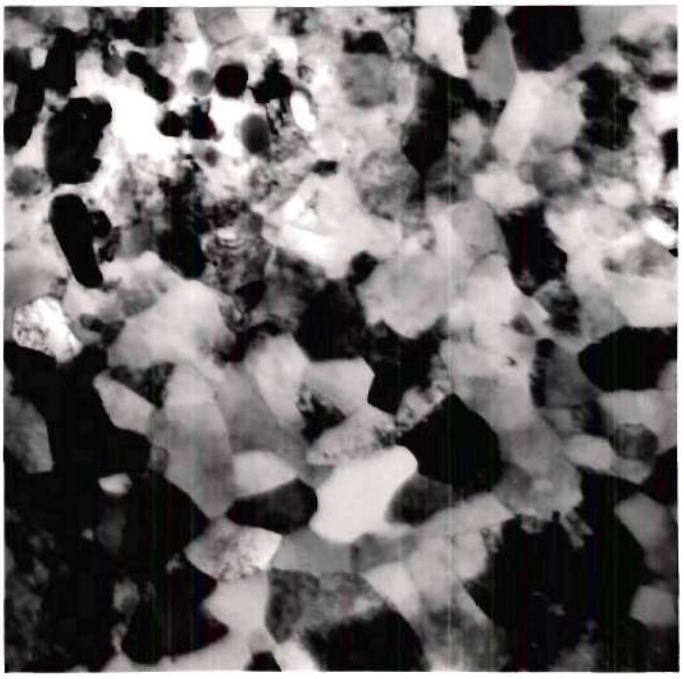

Figure 30. Transmission Electron Micrograph of "O" Temper 0.182 in. dia. Alloy Wire; 20,000X.

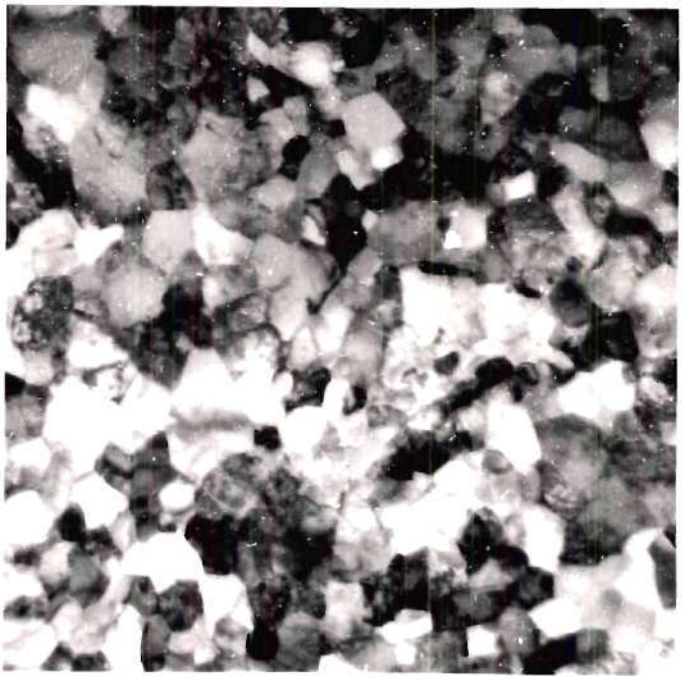

Figure 31. Transmission Electron Micrograph of "O" Temper 0.102 in. dia. Alloy Wire; 20,000X.

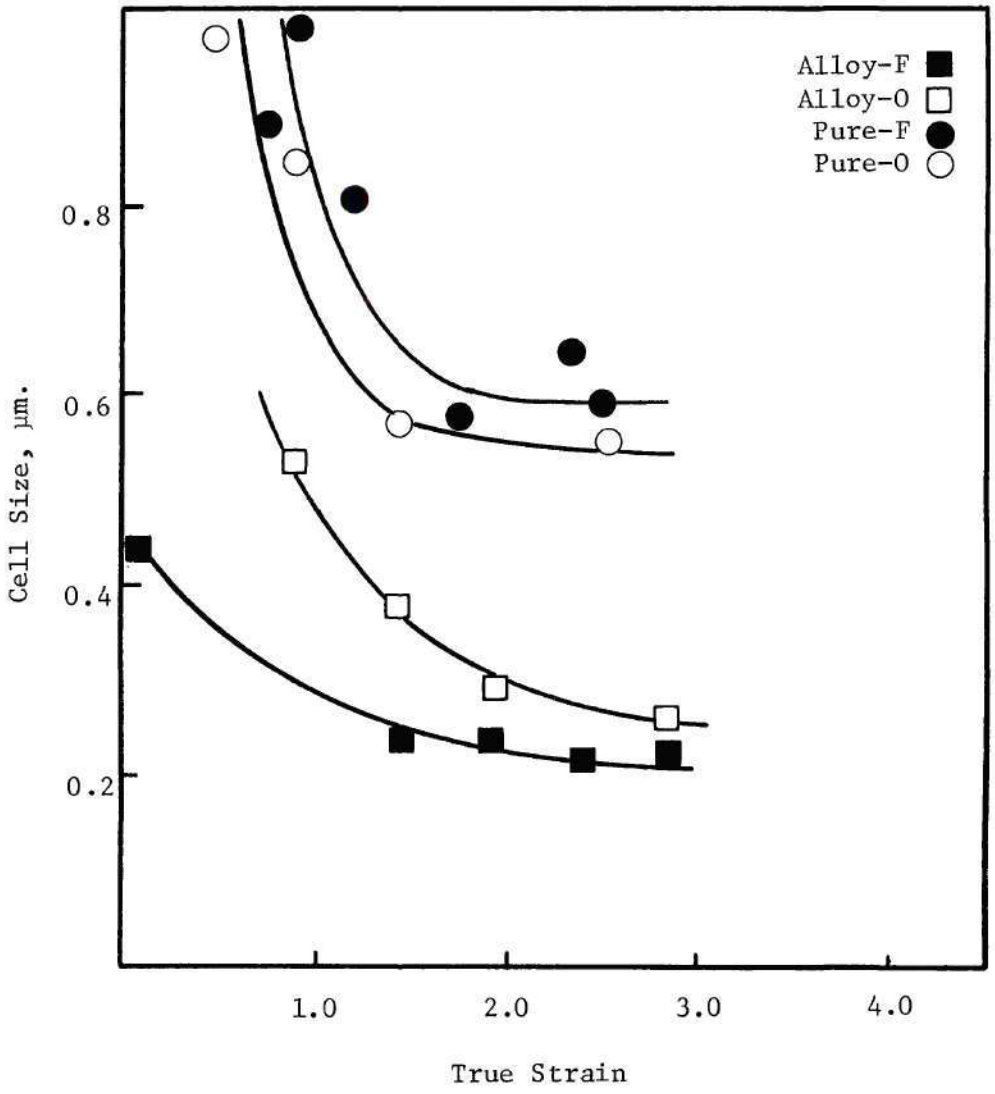

Figure 32. Cell Size vs. Strain Curves for Pure Aluminum and Al-Fe-Cu Alloy in "F" and "O" Temper Conditions.

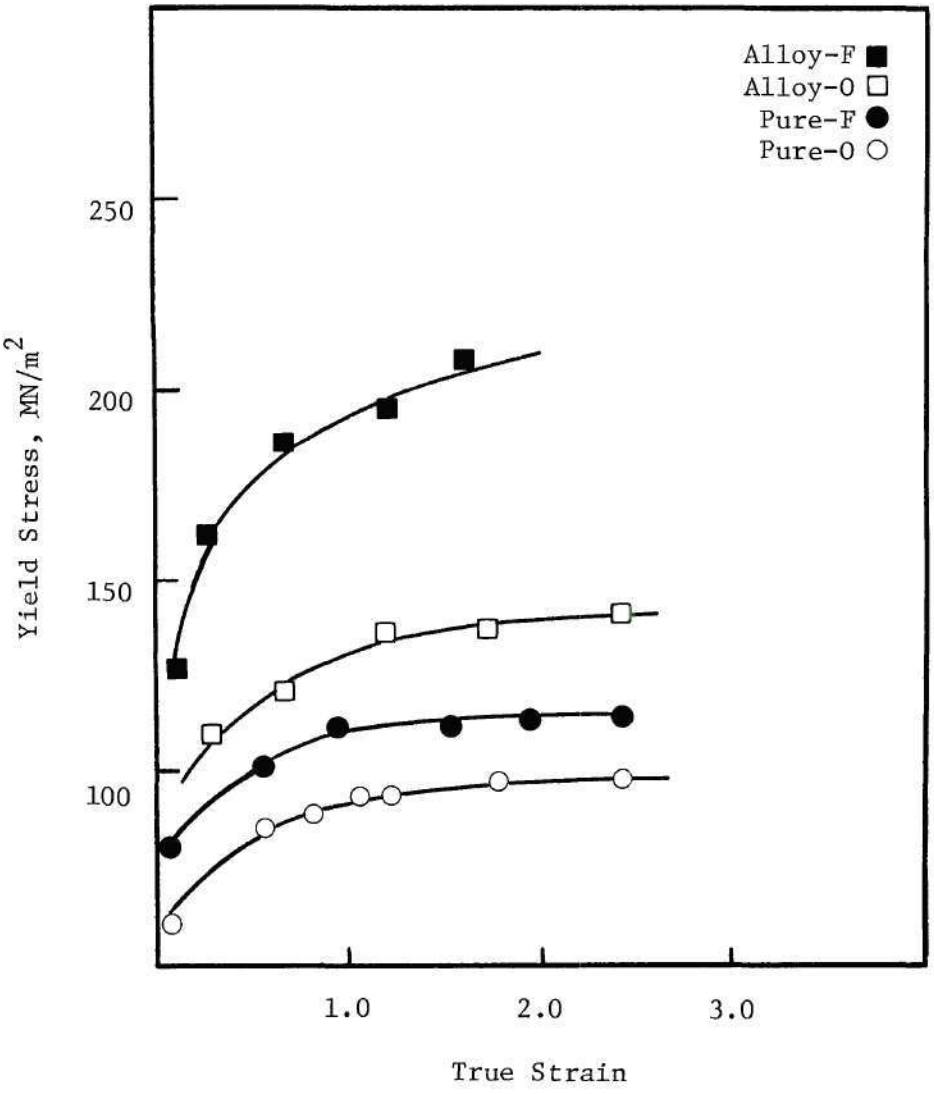

Figure 33. Strain Hardening Curves for Pure Aluminum and Al-Fe-Cu Alloy in "F" and "O" Temper Conditions.

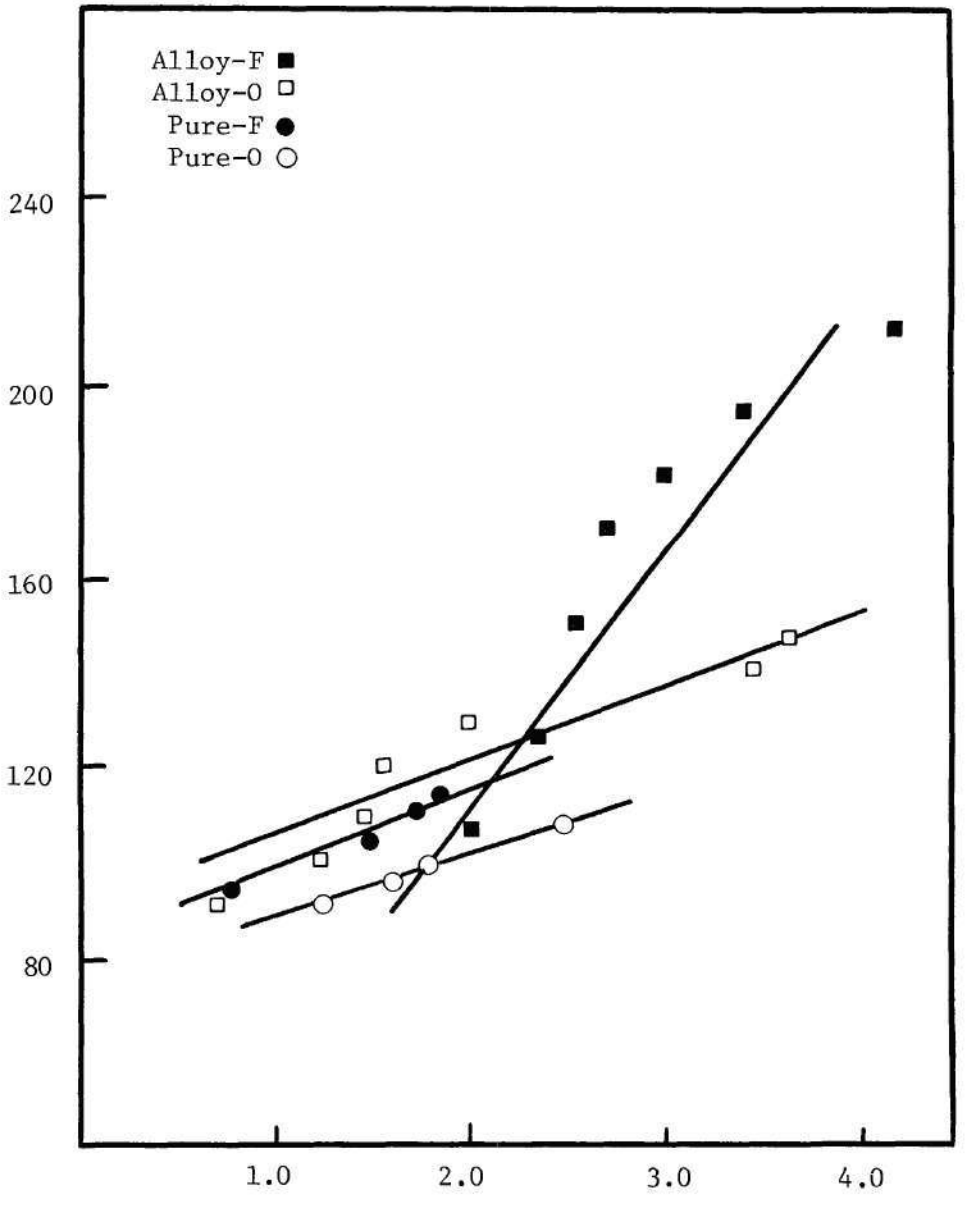

Figure 34. Hall-Petch Plots for Pure Aluminum and Al-Fe-Cu Alloy in "F" and "O" Temper Conditions.

Table 2. Values of σ_0 and k in Equation (4)

Material	σ_0	k
EC Aluminum[28]	0.55	0.50
Al-Fe-Mg[28]	0.34	0.88
Al-Fe-Co[28]	0.13	0.84
Fe[28]	0.34	1.19
Fe-Ti[28]	0.97	0.55
OFHC Cu[28]	-	1.30
99.99% Al (F-temper)	0.81	0.43
99.99% Al (O-temper)	0.75	0.38
Al-Fe-Cu (F-temper)	0.18	1.14
Al-Fe-Cu (O-temper)	0.87	0.43

CHAPTER V

CONCLUSIONS

The dilute Al-0.6Fe-0.2Cu conductor alloy and 99.99% aluminum show the following substructural strengthening characteristics during wire drawing to large strains at room temperature:

1. In Al-0.6Fe-0.2Cu subjected to wire drawing, the initial temper and microstructure has a large effect on the rate of work hardening, the rate of substructure refinement, and the effective strength of dislocation cell boundaries.

2. The "F" temper alloy (continuously cast and hot rolled) work hardens at a faster rate during wire drawing than the "O" temper (fully recrystallized), although the "O" temper shows a much faster rate of substructure refinement. The difference is attributed to the more effective cell boundary strengthening in the "F" temper material. An initial subgrain structure in the "F" temper material results in a different cell wall character during deformation.

3. Comparison with pure aluminum shows that the effect of initial microstructure is not pronounced unless alloying additions are present. The combined effect of soluble (Cu) and insoluble (Fe) additions causes the strength and substructure character during wire drawing to be more dependent on prior processing history.

BIBLIOGRAPHY

1. E. H. Chia and E. A. Starke, Jr., Met. Trans., 8A, (1977), 825.

2. R. E. Reed-Hill, Physical Metallurgy Principles, 2nd. edition, Van Nostrand Company, (1973), 284.

3. D. L. Holt, J. Appl. Phys., 41, (1970), 3197.

4. J. T. Moore and D. Kuhlmann-Wilsdorf, J. Appl. Phys., 41, (1970), 4411.

5. J. T. Moore and D. Kuhlmann-Wilsdorf, J. Appl. Phys., 42, (1971), 953.

6. J. T. Moore and D. Kuhlmann-Wilsdorf, J. Appl. Phys., 42, (1971), 3717.

7. J. T. Moore and D. Kuhlmann-Wilsdorf, J. Appl. Phys., 42, (1971), 3726.

8. J. T. Moore and D. Kuhlmann-Wilsdorf, Surface Science, 31, (1972), 456.

9. A. W. Thompson, Met. Trans., 8A, (1977), 833.

10. G. Langford and M. Cohen, Met. Trans., 6A, (1975), 901.

11. J. H. Cairnes, J. Clough, M. Dewey, and J. Nutting, J. Inst. Met., 99, (1971), 93.

12. E. O. Hall, Proc. Phys. Soc., 64, (1951), 747.

13. A. Crackness and N. Petch, Acta Met., 3, (1955), 186.

14. R. W. Armstrong, I. Codd, R. Douthwaite, N. Petch, Phil. Mag., 7, (1962), 45.

15. A. W. Thompson, M. A. Baskes, and W. F. Flanagan, Acta Met., 21, (1973), 1017.

16. R. J. McElroy and Z. Szkopiak, Internat. Met. Rev., 17, (1972), 175.

17. H. J. Rack and M. Cohen, Mat. Sci. Eng., 6, (1970), 320.

18. C. M. Young and O. D. Sherby, J. Iron Steel Inst., 211, (1973), 640.

19. M. Staker and D. Holt, Acta Met., 20, (1972), 569.

20. J. Fujita and M. Tabata, Acta Met., 21, (1973), 355.

21. H. J. Rack and M. Cohen, Frontiers in Materials Science, Dekker, New York, (1976), 365.

22. J. D. Baird and C. R. Mackenzie, J. Iron Steel Inst., 202, (1964), 427.

23. F. J. Herbert, K. M. Olsen, T. D. Schlaback, Wire Journal, 8, (1970), 51.

24. J. T. Barnby and E. Smith, Acta Met., 12, (1964), 1353.

25. M. VonHeimendahl and G. Thomas, Trans. Met. Soc. AIME, 230, (1964), 1521.

26. R. S. Goodrich and G. S. Ansell, Acta Met., 12, (1964), 1097.

27. L. F. Mondolfo, Aluminum Alloys: Structure and Properties, Butterworths, (1971), 490.

28. D. Kalish and B. G. LeFevre, Met. Trans., 6A, (1975), 1321.